Am J Transl Res 2019;11(3):1359-1373
www.ajtr.org /ISSN:1943-8141/AJTR0086816

*Original Article*

# Down-regulation of intracellular reactive oxygen species attenuates P-glycoprotein-associated chemoresistance in Epstein-Barr virus-positive NK/T-cell lymphoma

Young-Sun Nam[1,2,3], Keon-Il Im[1,3], Nayoun Kim[1,3], Yunejin Song[1,2,3], Jun-Seok Lee[1,2,3], Young-Woo Jeon[1,3,4], Seok-Goo Cho[1,2,3,4]

*[1]Institute for Translational Research and Molecular Imaging, [2]Department of Biomedicine and Health Sciences, The Catholic University of Korea, College of Medicine, Korea; [3]Laboratory of Immune Regulation, Convergent Research Consortium for Immunologic Disease (CRCID), [4]Department of Hematology, Catholic Blood and Marrow Transplantation Center, Seoul St. Mary's Hospital, The Catholic University of Korea, College of Medicine, Seoul, Korea*

Received October 16, 2018; Accepted January 29, 2019; Epub March 15, 2019; Published March 30, 2019

**Abstract:** Epstein-Barr virus (EBV)-positive extranodal NK/T-cell lymphoma is a rare and highly aggressive disease with a poor prognosis and strong resistance to anti-cancer drugs. Reactive oxygen species (ROS) are closely related to tumorigenesis and P-glycoprotein (P-gp) is highly expressed in various cancers. However, the exact relationship between ROS and P-gp in EBV-positive lymphoma remains unclear. In this study, we demonstrated that EBV latent infection induced intracellular ROS production and increased ROS levels triggered elevated P-gp expression, which resulted in strong resistance to existing anti-cancer drugs in EBV-positive lymphoma cell lines and in patients' tissue samples. We also verified that regulation of intracellular ROS reduced P-gp expression and function via inhibition of STAT1 phosphorylation. These results indicate that treatment with a ROS scavenger is a potential therapeutic strategy to overcome resistance to anti-cancer drugs by downregulating the expression of P-gp in EBV-positive NK/T-cell lymphoma.

**Keywords:** Epstein-Barr virus (EBV), extranodal NK/T-cell lymphoma (ENKTCL), reactive oxygen species (ROS), multi-drug resistance (MDR), P-glycoprotein (P-gp)

## Introduction

Epstein-Barr virus (EBV) is a human gammaherpes virus that exhibits three major latencies; I, II, and III and has been implicated in various tumors including lymphoma and gastric carcinoma [1-3]. Extranodal NK/T-cell lymphoma (ENKTCL), of which more than 95% of cases are EBV positive, shows a very poor prognosis and is characterised by distinct clinicopathological features including a low survival rate, metastasis [4], systemic inflammation [5] and drug resistance [4, 6]. It has been reported that various molecules are correlated with the poor prognosis and cell signalling pathways associated with an abnormal status in ENKTCL. EBV infection induces phosphorylation of molecules in the NF-κB, MAPK and JAK/STAT signalling pathways, resulting in tumor cell proliferation, angiogenesis and immune suppression [4, 7]. Patients with ENKTCL also showed mutations and/or methylation of, tumor suppressor genes including PRDM1, ATG5, AIM1 [8], FOXO3 and HACE1 [9]. In clinical practice, ENKTCL is highly resistant to the existing anti-cancer drugs including anthracycline-based regimens such as CHOP (cyclophosphamide, doxorubicin, vincristine and prednisolone). NK/T-cell lymphoma exhibits a multidrug-resistant (MDR) phenotype because of highly expressed P-glycoprotein (P-gp) [10]. To overcome this problem, MDR-independent drugs specifically designed for ENKTCL are now used. Therefore, concurrent chemo-radiotherapy regimens involving non-anthracycline chemotherapy using ifosfamide can improve treatment outcomes in patients by reducing local and systemic relapse rates, as explained in our previous report [11]. Also, to

overcome the immunological limitations of ENKTCL, we have been investigating other therapies using interferon alpha-2a [12] and EBV-specific cytotoxic T cells [13]. However, because there is still no complete cure, critical needs remain in the clinical treatment of ENKTCL.

In EBV-associated lymphoma, it has been reported that high ROS levels induced by EBV cause poor prognosis via deregulation of enzymes including catalase and peroxidase [14-16], gene instability [17-19] and modification of signalling pathways involved in anti-apoptotic effects and cell proliferation including NF-κB, MAPK and JAK/STAT [20-23]. Clinically, ENKTCL exhibits vascular damage and necrosis, which are closely related to high levels of ROS.

MDR is the major obstacle in cancer chemotherapy. Many cancers present resistance to anti-cancer drugs through the expression of P-gp, translated from the multidrug resistance protein 1 (*MDR1*) gene, which functions in an energy-dependent manner [24]. In various organs, P-gp expression induces the efflux of anti-cancer drugs. It has been reported that high levels of ROS induce P-gp expression [25, 26], hypoxia-inducible factor-1 (HIF-1) activation, nuclear translocation of NF-κB [27] and multicellular tumor spheroids [28] in various tumors. Patients with ENKTCL are positive for both P-gp and MDR1 mRNA and patients with high P-gp expression had poorer outcomes after chemotherapy alone [10]. In addition, it was demonstrated that EBV infection caused chemotherapy resistance through P-gp expression in EBV-positive T cell lymphoproliferative disease [29]. However, the direct mechanism of increased P-gp in ENKTCL remains unclear.

In this study, we examined the direct molecular pathological mechanisms of P-gp expression in EBV-positive NK/T-cell lymphoma, whether increased ROS induced by EBV infection upregulate the expression and function of P-gp, and which signalling pathways are involved in this process. We also investigated the possible use of the ROS scavenger NecroX-5 as an anti-cancer complement via its regulation of MDR in ENKTCL.

## Materials and methods

### *Cell lines and materials*

Of the cell lines used in this study, H9, Jurkat and Karpas-299 cells are EBV-negative T cell lines. NKL and KHYG-1 are EBV-negative NK cell lymphoma cell lines, and NK-92, NK-YS, KAI3, HANK-1 and SNK-6 are EBV-positive NK cell lymphoma cell lines. H9 cell is purchased from Korean Cell Line Bank (Seoul, Republic of Korea), KHYG-1 and KAI3 cells from the Japanese Collection of Research Bioresources Cell Bank (Osaka, Japan), and NK-92 cells from the American Type Culture Collection (Manassas, VA, USA). Jurkat, Karpas-299, H9, NKL, KHYG-1 and KAI3 cells were grown in RPMI 1640 medium (Gibco, Carlsbad, CA, USA) containing 2 mM L-glutamine (Gibco), 1% 2-mercaptoethanol (Gibco), 1% antibiotics (10 U/mL penicillin and 10 g/mL streptomycin; Gibco), 10% heat-inactivated foetal bovine serum (FBS; Gibco) and 200 U/mL recombinant human IL-2 (rhIL-2, PeproTech, London, UK) were added to NKL, KHYG-1 and KAI3. NK-YS cells were cultured in IMDM medium (Gibco) containing 1% antibiotics (10 U/mL penicillin and 10 g/mL streptomycin), 10% heat-inactivated FBS and 100 U/mL rhIL-2. HANK-1 and SNK-6 cells were grown in RPMI 1640 medium containing 1% 2-mercaptoethanol (Gibco), 10% human serum (Sigma-Aldrich, St. Louis, MO, USA) and 100 U/mL and 700 U/mL rhIL-2, respectively. NK-92 cells were cultured in alpha-MEM medium (Gibco) containing 2 mM L-glutamate (Gibco), 1.5 g/L sodium bicarbonate (Gibco), 0.2 mM inositol (Sigma-Aldrich), 0.1 mM 2-mercaptoethnaol (Gibco), 0.02 mM folic acid (Sigma-Aldrich), 12.5% FBS, 12.5% horse serum (Gibco) and 200 U/mL rhIL-2 (PeproTech). NecroX-5 ($C_{25}H_{31}N_3O_3S{\cdot}2CH_4O_3S$) was purchased from Enzo Life Sciences (Farmingdale, NY, USA).

### *ROS assay*

A solution of 2',7'-dichlorofluorescein diacetate (DCFDA; Sigma-Aldrich) in methanol (Bio-Lab, Jerusalem, Israel) was added at a final concentration of 2 μM to cell lines in phosphate-buffered saline (PBS). After a 40-min incubation at 37°C in a humidified atmosphere of 5% $CO_2$ in air, the cells were washed and resuspended in PBS.

### *Cell Counting Kit-8 (CCK-8) assay*

Cell growth was assessed using the CCK-8 (Dojindo, Rockville, MD, USA) assay according to the manufacturer's protocol. Briefly, $5 \times 10^4$ lymphoma cells were dispensed in 100 μL culture medium in 96-well plates, and various

doses of anti-cancer drugs were diluted in 100 μL. Cultures were maintained at 37°C in a 5% $CO_2$ atmosphere. After 24 or 48 h, 20 μL CCK-8 solution were added to each well, and the plate was incubated for 1-4 h in a $CO_2$ incubator. The optical density was measured at 450 nm using a microplate reader.

*Flow cytometric analysis*

To investigate P-gp expression, lymphoma cells were immunostained with anti-human CD243 PE (P-gp; eBioscience, San Diego, CA, USA) for 30 min at 4°C. After staining, lymphoma cells were washed with staining buffer and resuspended in staining buffer. To investigate signalling pathways, lymphoma cells were pre-treated with 20 μM NecroX-5 for 30 min. Cells were washed and cultured at 37°C for 16 h. Intracellular staining with phospho-STAT1, STAT3, ERK1/2 and NF-κB (BioLegend, San Diego, CA, USA) was performed using an intracellular staining kit (eBioscience) according to the manufacturer's protocol. Flow cytometric analysis was performed on the FACS_LSR Fortessa (BD Pharmingen, San Diego, CA, USA) using FlowJo software (TreeStar, Ashland, OR, USA).

*Western blot analysis*

Total protein was collected from cells pre-treated with or without 20 μM NecroX-5. Cells were homogenized by lysis buffer with a protease/phosphatase inhibitor cocktail (Cell signalling, Danvers, MA) and western blotting was performed. The primary antibody used was rabbit antibodies to P-gp (1:1000, ERP10364-53; Abcam, Cambridge, UK) and β-actin (1:2000, Cell signalling). After overnight incubation in 4°C, HRP-conjugated secondary antibody was added. After washing with Tris-buffered saline and Twenn 20, the hybridized bands were detected using an enhanced chemiluminescence (ECL) detection kit (Amersham Pharmacia Biotech, Buckinghamshire, UK).

*Rhodamine 123 (Rho123) accumulation assay*

NKL, NK-92 and NK-YS cells ($5 \times 10^5$) were grown on 24-well plates and pre-treated with NecroX-5 for 1 h at 37°C. The cells were then washed with PBS and stimulated with 125 μM $H_2O_2$ for 16 h. Rho123 (0.5 μg/mL) was added, and cells were incubated at 37°C for an additional 1 h in the presence or absence of $H_2O_2$. The cells were harvested, and the concentration of Rho123 was measured by flow cytometric analysis.

*EBV-encoded small RNA (EBER) in situ hybridization and immunohistochemistry (IHC)*

Patient biopsied lymphoma tissues were formalin-fixed, paraffin-embedded and sectioned at a thickness of 4 μm. Staining for EBERs was performed using the INFORM EBERs probe (Ventana, Tucson, AZ, USA) according to the manufacturer's protocol. For IHC, slides were dehydrated using xylene and ethanol, and antigen retrieval and blocking were performed. Antibodies targeting P-gp (Abcam) was diluted 1:50 and then incubated with the slides at 4°C overnight. Anti-rabbit IgG-HRP (Santa Cruz Biotechnology) was used as the secondary antibody, and the slides were incubated at room temperature for 2 h. Signals were detected using the REAL EnVision detection system, peroxidase/DAB+ (Dako, Santa Clara, CA, USA). Counterstaining was performed using Mayer's haematoxylin (Dako) for 1 min at room temperature.

*Real-time reverse transcription PCR (RT-PCR)*

Total RNA was extracted using TRIzol-LS reagent (Invitrogen). Total RNA was reverse transcribed using ReverTra Ace qPCR RT master mix (Toyobo, Osaka, Japan) according to the manufacturer's protocol. RT-PCR was performed using the IQ SYBR Green Super Mix and CFX 96 real-time system (Bio-Rad, Hercules, CA, USA) under the following conditions: denaturation at 95°C for 3 min, annealing at 58°C for 30 s, followed by extension at 72°C for 30 s. For quantification, relative mRNA expression of specific genes was calculated using the $2^{-\Delta\Delta Ct}$ method, after normalization to β-actin expression. The following gene-specific primers were used: β-actin (forward: 5'-GAA ATC GTG CGT GAC ATCAAA G-3'; reverse: 5'-TGT AGT TTC ATG GAT GCC ACA G-3') and MDR1 (forward: 5'-CAG GAA CCT GTA TTG TTT GCC ACC AC-3'; reverse: 5'-TGC TTC TGC CCA CCA CTC AAC TG-3').

*Statistical analysis*

All statistical analysis was performed using SPSS statistical software package (SPSS, Chicago, IL, USA). Statistical significance was

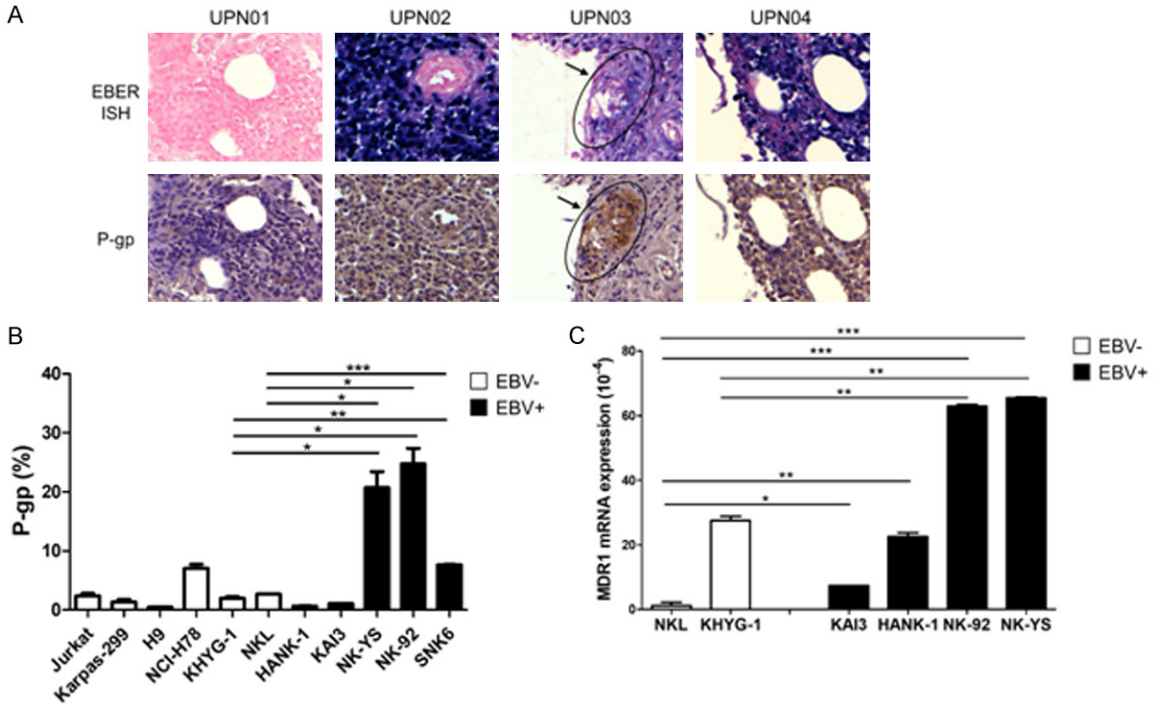


**Figure 1.** Expression of P-gp in EBV-associated lymphoma patients' tissues and cell lines. A. Patients with ENKTCL weakly expressing EBERs showed low expression level of P-gp (UPN01), however, patients' tissues with strong EBER expression exhibited P-gp (ERP10364-53; UPN02, 03 and 04) analysed by in situ hybridization (ISH) and immunohistochemistry (IHC). B. P-gp expression in various T- or NK-cell lymphoma cell lines analysed by flow cytometry. C. mRNA expression level of MDR1 in lymphoma cell lines analysed by real-time PCR. Compared to EBV-negative, EBV-positive lymphoma cells showed high expression of P-gp protein and MDR1 gene. White and black bars indicate EBV-negative and EBV-positive cells, respectively. *P < 0.05, **P < 0.01, ***P < 0.001 vs. indicated group.

determined using student's two-tailed t-test and one-way analysis of variance (ANOVA) with Bonferroni correction for multiple comparisons. In all analysis, data are presented as means ± SD and *P*-values < 0.05 were considered to indicate significance.

## Results

### *P-gp expression and ROS levels are elevated in EBV-positive NK/T-cell lymphoma*

To determine the association between EBV and P-gp, EBV infection and P-gp expression were measured in lymphoma tissues from ENKTL patients using EBER *in situ* hybridization and IHC, respectively. Patients with negative for EBV infection showed low expression of P-gp (**Figure 1A**, UPN01). Interestingly, P-gp was highly expressed in the tissue areas with strong EBER expression (**Figure 1A**, UPN02, 03 and 04). Therefore, to examine the association between EBV and P-gp, firstly we investigated P-gp expression in various EBV-associated NK/T-cell lymphoma cell lines using flow cytometry analysis. EBV-negative T cell lymphoma cell lines (H9), EBV-negative NK cell lymphoma cell lines (KHYG-1 and NKL) and EBV-positive NK cell lymphoma cell lines (HANK-1 KAI3, NK-YS, NK-92 and SNK-6) were used. Interestingly, compared with EBV-negative cells, EBV-positive cells showed higher P-gp expression. In NK-YS and NK-92 cells, P-gp expression was more than 10 times higher than that in KHYG-1 and NKL cells (**Figure 1B**). The MDR1 mRNA level was also detected to confirm P-gp expression. As with P-gp expression, EBV-positive lymphoma cell lines, including NK-92 and NK-YS cells, showed higher MDR1 mRNA expression (**Figure 1C**). Although KHYG-1 showed higher MDR1 mRNA levels compared to two EBV-positive cell lines; KAI3 and HANK-1, P-gp expression was lower compared to EBV-positive cells.

Next, to investigate the relationships among EBV, ROS and P-gp, ROS levels in EBV-associated cell lines were measured by flow cytom-

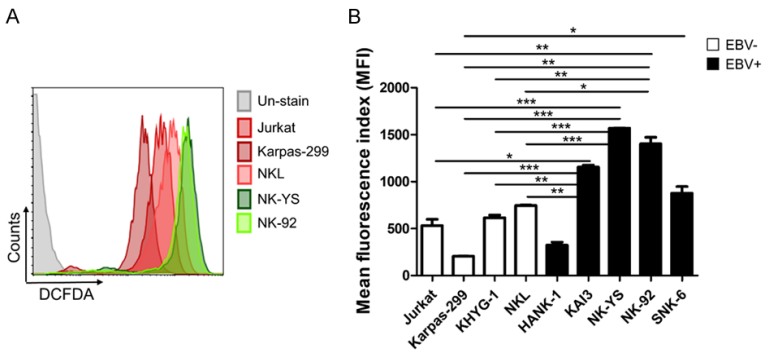


**Figure 2.** ROS levels in EBV-associated lymphoma cell lines. A. Intracellular ROS levels shown by the histogram using flow cytometry. B. Graph of MFI levels. Compared with EBV-negative cell lines, most EBV-positive T and NK cell lines showed higher MFI values. In some EBV-positive cell lines, intracellular ROS levels were more than threefold higher than those in EBV-negative cells. *P < 0.05, **P < 0.01, ***P < 0.001 vs. indicated group.

etry using DCFDA. As shown in the histogram, compared with EBV-negative cells (Jurkat and Karpas-299; T cells and NKL; NK cells), EBV-positive NK-YS and NK-92 cells had higher ROS levels (**Figure 2A**). The mean fluorescence index (MFI) of DCFDA in the cell lines was also examined. Compared with EBV-negative cells, EBV-positive cells showed significantly higher ROS levels. Particularly, NK-YS and NK-92 cells had more than twofold higher ROS levels than those of EBV-negative cells (**Figure 2B**). These data indicate that although there are differences in cell lines, EBV infection induced hypoxic conditions and increased intracellular ROS levels up-regulated P-gp expression.

*Inhibition of intracellular ROS levels downregulates P-gp expression*

To investigate the direct relationship between ROS and P-gp, both EBV-negative and -positive NK cell lymphoma cell lines were treated with NecroX-5, a free radical scavenger. This indole backbone-based synthetic compound exhibited antioxidant effects in various disease models [30, 31] including graft versus host disease in our previous studies [32]. Cells were treated with 0, 10, 20 and 40 μM NecroX-5 for 2 hours, then washed and cultured for 16 hours. As shown in **Figure 3A**, ROS levels tended to decrease after treatment with NecroX-5, in a dose-dependent manner. Interestingly, Necrox-5 regulated ROS levels more significantly in EBV-positive lymphoma cell lines. After 16 hours, P-gp expression was detected by flow cytometry. In EBV-negative cell lines, NecroX-5 downregulated P-gp expression to some degree (**Figure 3B**). Although P-gp expression was reduced in NKL cells, NecroX-5 had less effect on P-gp regulation, because of the low P-gp expression in controls. In all EBV-positive cell lines, all doses of NecroX-5 downregulated P-gp expression (**Figure 3B**). NecroX-5 at 40 μM decreased P-gp from 7.62% to 3.51% and from 19.2% to 6.69% in SNK-6 and NK-92 cell lines, respectively. Interestingly, P-gp expression was dramatically decreased in NK-YS cells, from 18.9% to 1.66%, even at the lowest dose of NecroX-5 used. P-gp expression was also regulated by NecroX-5 in HANK-1 cells; however, because P-gp expression in NecroX-5-untreated cells was already low, the changes were not significant and it seems that the most effective dose of NecroX-5 appeared to differ from cell to cell. In NK-92 and NK-YS cells, 40 μM was the most effective dose for both ROS regulation and P-gp downregulation. In addition to these data, we confirmed that NecroX-5 was able to decrease P-gp expression analysed by western blot analysis in NKL, NK-92, NK-YS and HANK-1 cells (Figure S1). Similar to flow cytometry data, cell lines with high expression of P-gp; NK-92 and NK-YS showed decreased P-gp level after NecroX-5 treatment and in NKL, P-gp expression was rarely detected both in NecroX-5 untreated and pre-treated group. These results suggest that NecroX-5 decreased P-gp expression by regulating ROS.

*P-gp function is attenuated by the regulation of intracellular ROS*

To investigate whether ROS regulation directly affects P-gp function in EBV-positive lymphoma, we assessed accumulation of Rho123, the substrate of P-gp located in the mitochondria, after NecroX-5 treatment. In the case of low expression of P-gp, Rho123 was accumulated in intracellular space and in the case of high expression of P-gp, P-gp pumped out Rho123, therefore, Rho123 accumulation was reduced resulted in decreased fluorescence analysed by flow cytometry. We pre-treated lymphoma

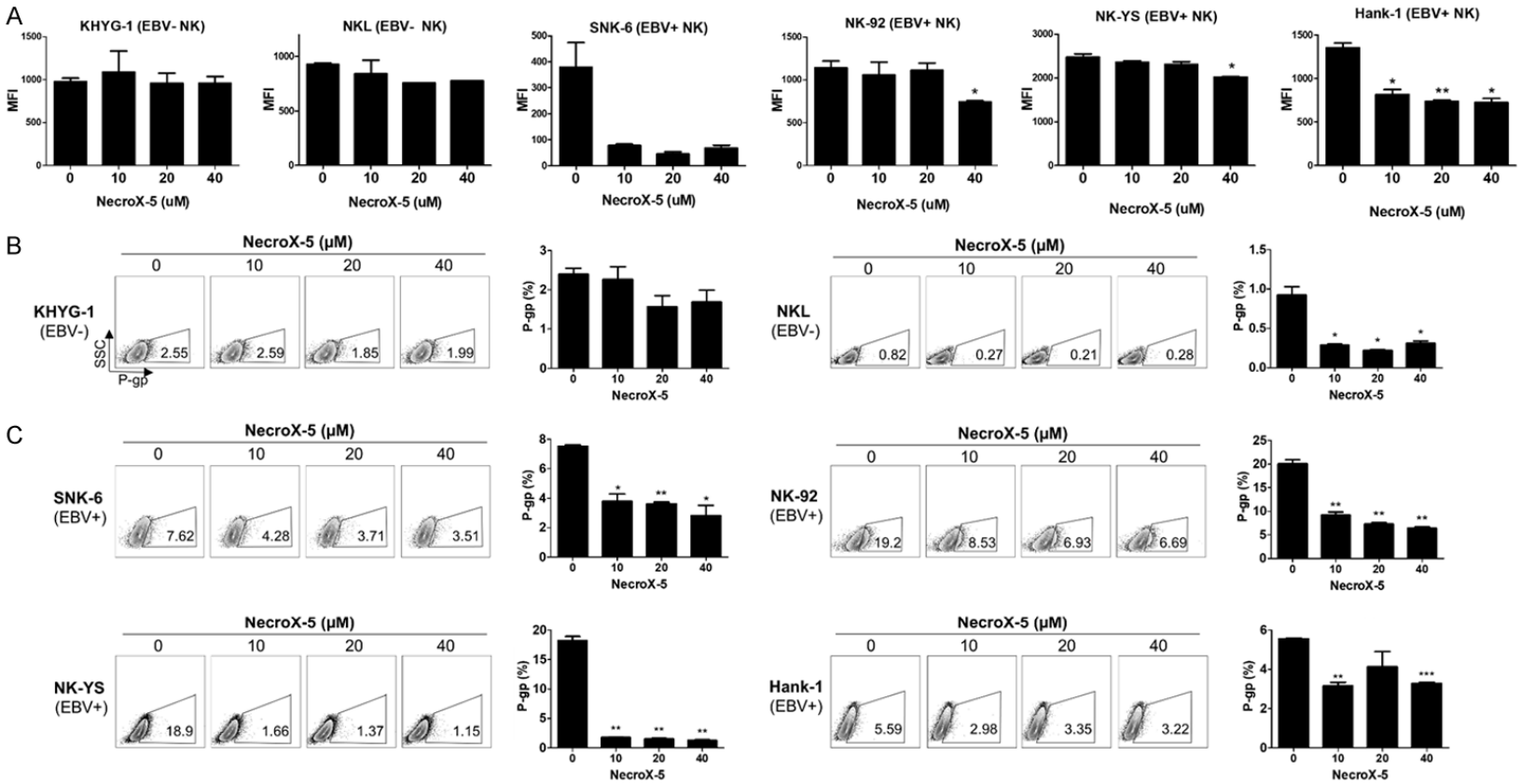


**Figure 3.** The effects of ROS inhibition in P-gp expression. A. In EBV-negative cell lines, NecroX-5 did not affect intracellular ROS levels, whereas in EBV-positive cells, NecroX-5 regulated intracellular ROS in a dose-dependent manner. B. EBV-negative KHYG-1 and NKL cells were treated with various doses of NecroX-5 for 2 h. After 16 h of culture, P-gp expression was measured by flow cytometry. NecroX-5 regulated P-gp expression in NKL cells only. C. Compared to EBV-negative cell lines, dramatic regulation was shown at all doses of NecroX-5 in EBV-positive NK cell lymphoma cell lines including SNK-6, NK-92, NK-YS and HANK-1. *P < 0.05, **P < 0.01, ***P < 0.001 vs. control group.

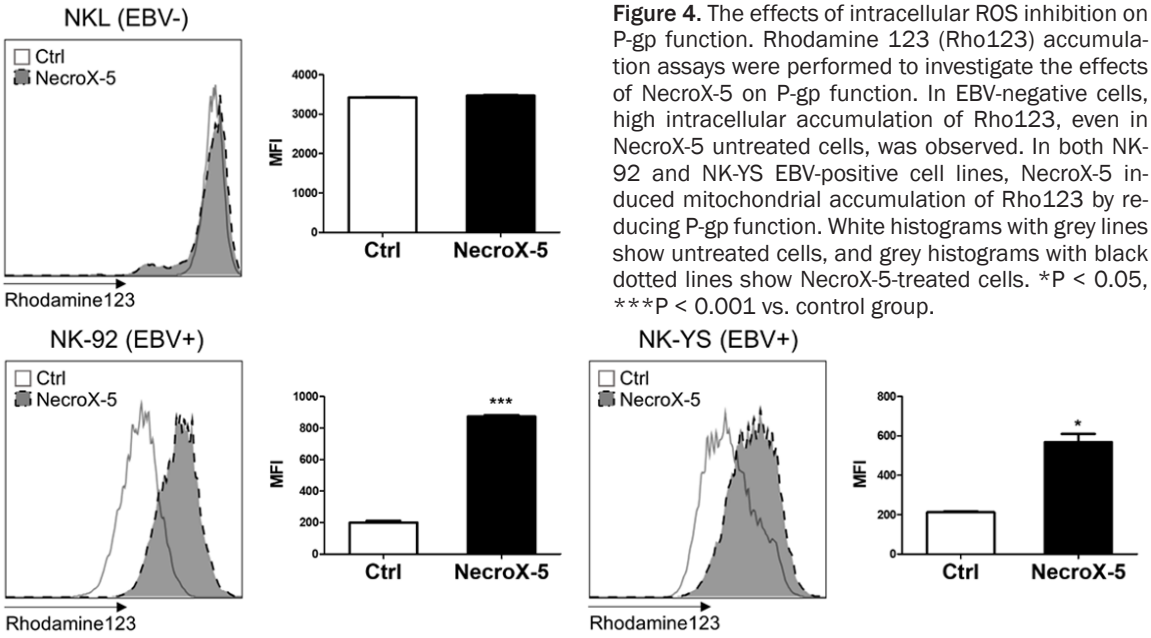


**Figure 4.** The effects of intracellular ROS inhibition on P-gp function. Rhodamine 123 (Rho123) accumulation assays were performed to investigate the effects of NecroX-5 on P-gp function. In EBV-negative cells, high intracellular accumulation of Rho123, even in NecroX-5 untreated cells, was observed. In both NK-92 and NK-YS EBV-positive cell lines, NecroX-5 induced mitochondrial accumulation of Rho123 by reducing P-gp function. White histograms with grey lines show untreated cells, and grey histograms with black dotted lines show NecroX-5-treated cells. *P < 0.05, ***P < 0.001 vs. control group.

cells with NecroX-5 and incubated at 37°C with Rho123. In EBV-negative cells, Rho123 showed high intracellular accumulation regardless of NecroX-5 treatment (**Figure 4**, upper panel) because of the lower expression of P-gp. In contrast, as shown in the lower panel of **Figure 4**, Rho123 showed high intracellular accumulation in EBV-positive NK cells. In NK-92 cells, the MFI for intracellular Rho123 was more than fourfold higher after NecroX-5 treatment. NecroX-5 also increased intracellular Rho123 accumulation in NK-YS cells, but not as dramatically as in NK-92 cells. The MFI of Rho123 was approximately threefold higher after NecroX-5 treatment. These results suggest that NecroX-5 directly reduced P-gp function.

*Regulation of ROS promotes the cytotoxicity of anti-cancer drugs*

Patients with EBV-positive NK/T-cell lymphoma are refractory to conventional anti-cancer drugs including P-gp-dependent drugs such as doxorubicin and cisplatin and P-gp-independent drugs including cyclophosphamide and methotrexate. To evaluate whether NecroX-5 increases the sensitivity to anti-cancer drugs, we treated EBV-negative and -positive lymphoma cell lines with various doses of NecroX-5. In EBV-negative cell lines, intracellular ROS inhibition affected cell viability in a dose-dependent manner (**Figure 5A**). A dose of 40 μM was sufficient to kill 50% of lymphoma cells. However, EBV-positive cell lines showed varying cytotoxicities toward NecroX-5. HANK-1 and SNK-6 cells showed similar patterns to those of EBV-negative cells. However, interestingly, two EBV-positive NK cell lines, NK-92 and NK-YS, which showed high expression of P-gp and ROS in previous experiments, were not significantly affected by NecroX-5 treatment. Next, we investigated the cytotoxic effects of anti-cancer drugs combined with NecroX-5 in EBV-positive cells (**Figure 5B**). In EBV-negative NKL cells, which showed low P-gp expression, four anti-cancer drugs (P-gp-dependent drugs doxorubicin and cisplatin and P-gp-independent drugs cyclophosphamide and methotrexate) showed high dose-dependent cytotoxic effects and even at the 1 μM dose of doxorubicin and methotrexate, half of the NKL cells were killed. However, there were no differences between NecroX-5-treated and -untreated cells. Interestingly, in EBV-positive NK-92 cells, P-gp-dependent cisplatin and two P-gp-independent drugs, cyclophosphamide and methotrexate, were ineffective regardless of NecroX-5 co-treatment. However, the cytotoxic effects of doxorubicin were significantly increased in NecroX-5-pre-treated cells even at low doses. Additionally, NecroX-5 pre-treated NK-YS cells were sensitive to doxorubicin, whereas they were dose-dependently sensitive to cisplatin regardless of NecroX-5 treatment. Cyclophosphamide and methotrex-

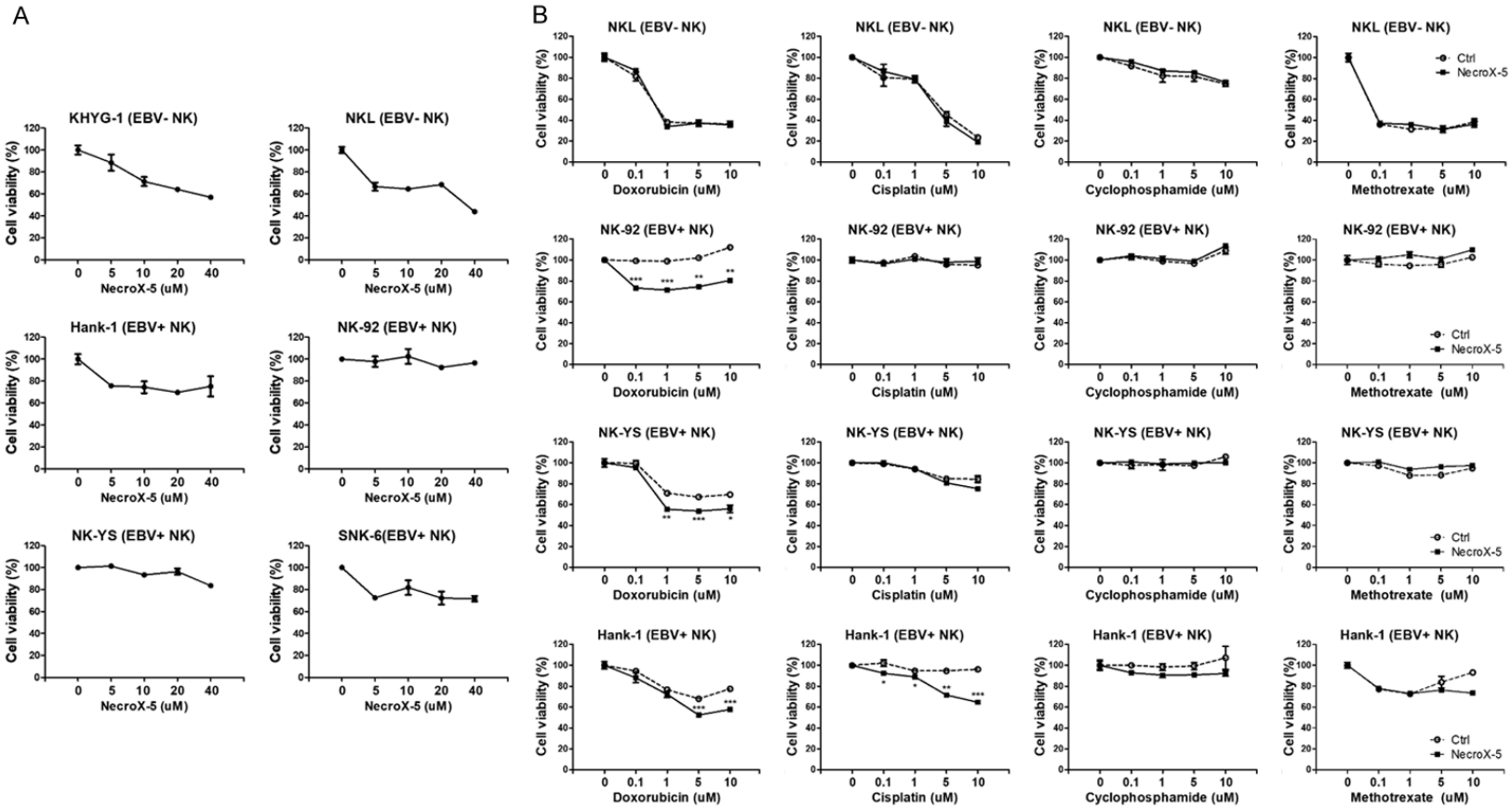


**Figure 5.** The cytotoxic effects of NecroX-5 alone or with anti-cancer drugs. CCK-8 assay measuring cell viability for investigating the cytotoxic effects of NecroX-5. A. Although the cytotoxic effects of NecroX-5 varied by cell line, all EBV-negative cells were sensitive to NecroX-5 alone. However, in most EBV-positive cell lines, NecroX-5 alone was not sufficient to kill lymphoma cells. B. Lymphoma cell lines pre-treated with 40 μM NecroX-5 for 1 hour were cultured with four anti-cancer drugs for 48 h. In EBV-positive NK cell lymphoma cells, NecroX-5 enhanced the cytotoxic effects of the P-gp-dependent anti-cancer drugs doxorubicin and cisplatin. Dotted lines with empty circles indicate untreated cells, and dark lines with full squares indicate cells pre-treated with NecroX-5. *P < 0.05, **P < 0.01, ***P < 0.001 vs. NecroX-5 non-treated group.

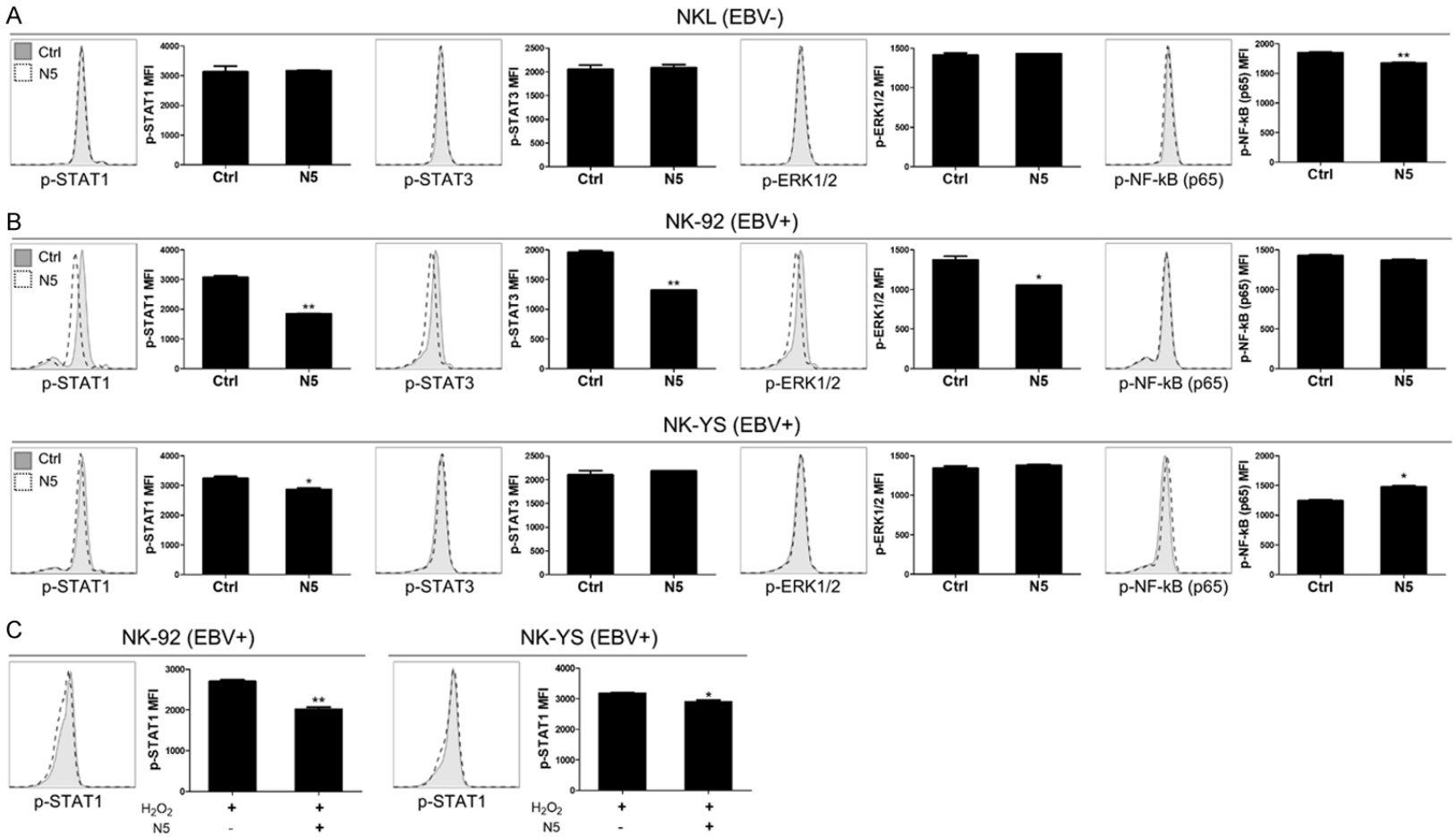


**Figure 6.** The involvement of STAT1 phosphorylation after inhibition of intracellular ROS. A. In NKL cells, phosphorylation of NF-κB, but not STAT1, STAT3 or ERK1/2, was inhibited by NecroX-5. B. In NK-92 cells, NecroX-5 downregulated STAT1, STAT3, ERK1/2 and NF-κB expression. In NK-YS, only the STAT1 signalling pathway was regulated and NecroX-5 upregulated NF-κB phosphorylation. C. Under hypoxic conditions induced by $H_2O_2$ stimulation, STAT1 signalling was inhibited by NecroX-5. Grey histograms show untreated cells, and white histograms with dotted lines show NecroX-5-treated cells. *P < 0.05, **P < 0.01, ***P < 0.001 vs. NecroX-5 non-treated group.

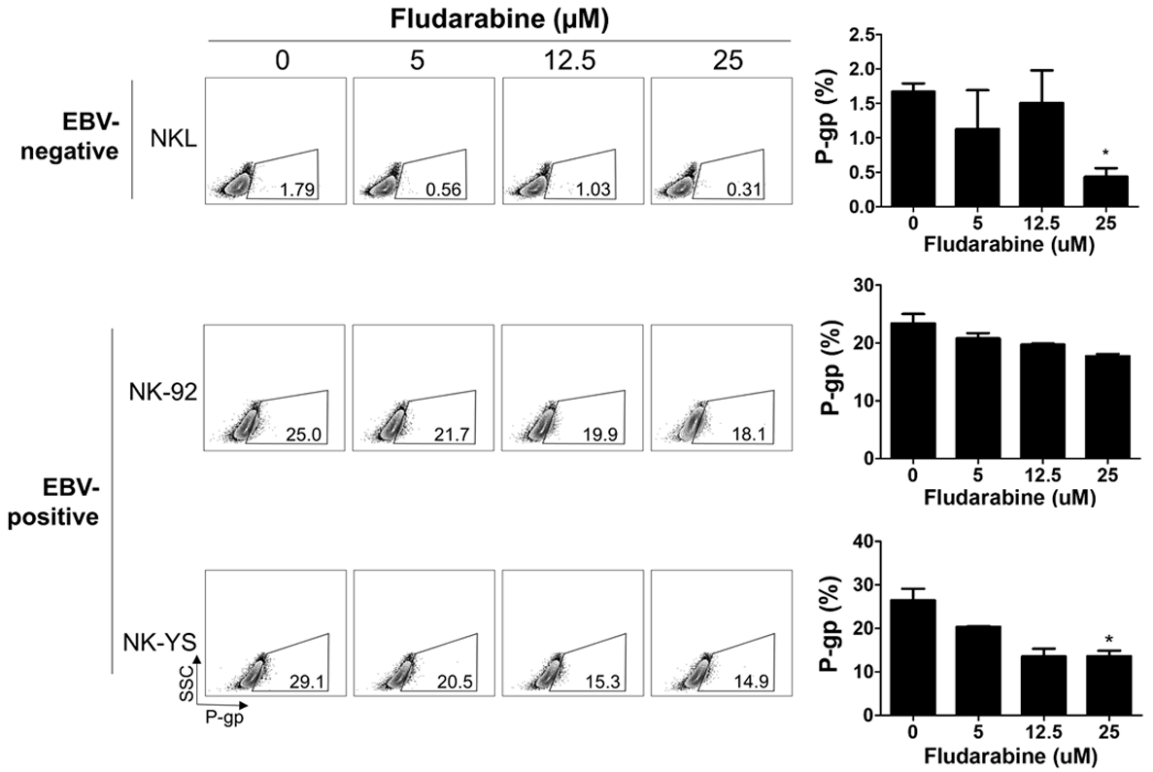


**Figure 7.** The effects of STAT1-specific inhibition using fludarabine on P-gp expression in EBV-positive NK cell lymphoma cells. To inhibit STAT1 directly, lymphoma cells were treated with various doses of fludarabine, and P-gp expression was subsequently measured by flow cytometry. Regardless of the EBV infection status, STAT1 inhibition downregulated P-gp expression in a fludarabine dose-dependent manner. However, the effects of P-gp downregulation were more significant in EBV-positive cells than EBV-negative because of the basal expression of P-gp. *P < 0.05 vs. NecroX-5 non-treated group.

ate were less effective in both the NecroX-5 pre-treated and untreated groups. Interestingly, HANK-1 cells pre-treated with NecroX-5 showed dramatically increased sensitivity to the P-gp-dependent drugs doxorubicin and cisplatin. From these data, we concluded that NecroX-5 induced sensitivity to conventional anti-cancer drugs especially in the case of P-gp-dependent drugs and it may provide a novel anti-cancer drug complement.

*Inhibition of STAT1 phosphorylation downregulates P-gp expression*

To investigate which signalling pathways are involved in regulating P-gp expression via NecroX-5 and whether there is a difference between EBV-negative and EBV-positive cell lines, NKL, NK-92 and NK-YS cells were pre-treated with various doses of NecroX-5 and stained for phospho-STAT1, STAT3, ERK1/2 and NF-κB. As shown in **Figure 6A**, there were no significant differences in STAT1, STAT3 or ERK1/2 phosphorylation after NecroX-5 treatment. Interestingly, NecroX-5 inhibited the phosphorylation of NF-κB (p65) in EBV-negative cells. In EBV-positive NK-92 cells, STAT1, STAT3, ERK1/2 and NF-κB phosphorylation were downregulated by NecroX-5 (**Figure 6B**, upper level). Both STAT1 and STAT3 phosphorylation were significantly decreased; the MFI of p-STAT1 decreased from 3073.5 to 1849.5 and that of STAT3 decreased from 1958.5 to 1323.5 following NecroX-5 treatment. The MFI of ERK1/2 phosphorylation was also downregulated from 1374 to 1055. Although NecroX-5 also inhibited NF-κB phosphorylation, this effect was not significant. In NK-YS cells, NecroX-5 did not affect the phosphorylation of STAT3 or ERK1/2 (**Figure 6B**, lower level). However, STAT1 phosphorylation was downregulated and NF-κB phosphorylation upregulated after NecrX-5 treatment. Therefore, we confirmed that NecroX-5 regulated STAT1 phosphorylation only in EBV-positive

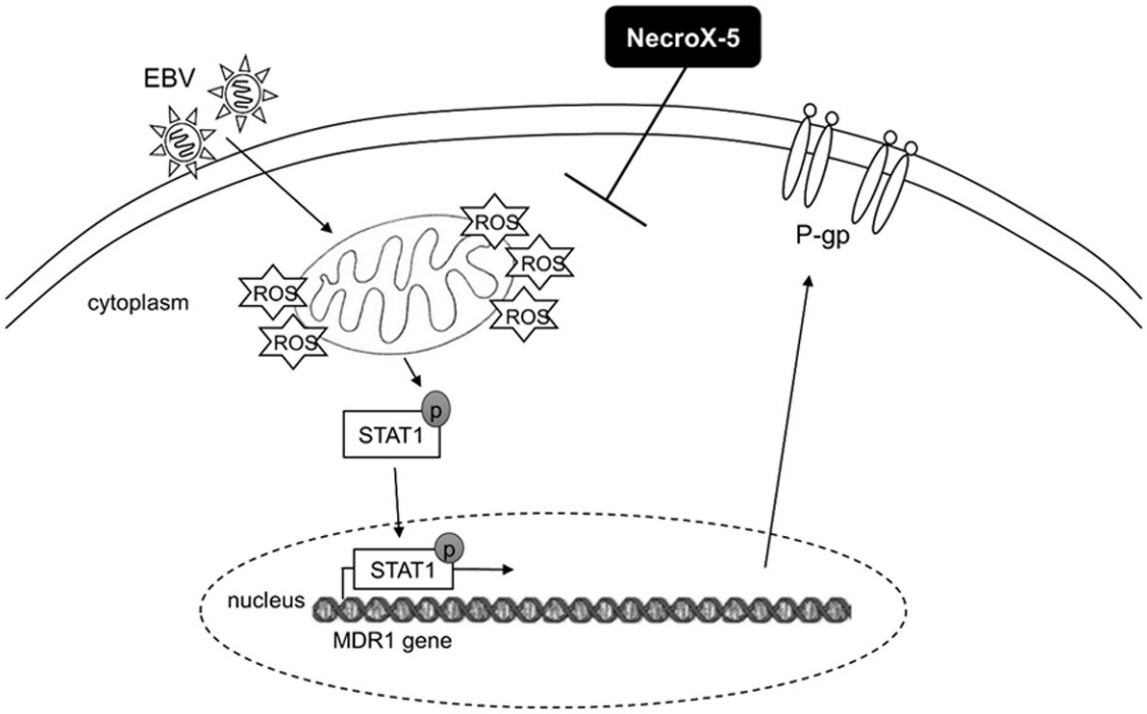


**Figure 8.** Schematic diagram of the relationships among EBV, ROS and P-gp, and the effects of NecroX-5 on P-gp regulation. After EBV infection, elevated ROS levels induce STAT1 phosphorylation, and phosphorylated STAT1 induces MDR1 expression, resulting in production of P-gp. NecroX-5 decreases P-gp expression by regulating intracellular ROS level.

lymphoma cells. To clarify whether NecroX-5 regulates the STAT1 signalling pathway under hypoxic conditions in EBV-positive lymphoma, we pre-treated cells with 20 μM NecroX-5 and stimulated them with $H_2O_2$ to establish hypoxic conditions. Interestingly, NecroX-5 significantly reduced STAT1 phosphorylation under hypoxic conditions in EBV-positive cells (**Figure 6C**). From these data, we determined that NecroX-5 regulated P-gp expression via the STAT1 signalling pathway.

Therefore, to clarify the relationship between STAT1 phosphorylation and P-gp expression, we used the STAT1-specific inhibitor fludarabine. Lymphoma cells were treated with various doses of fludarabine for 2 h. After inhibiting STAT1 phosphorylation with fludarabine, P-gp expression was reduced not only in EBV-positive but also EBV-negative cells (**Figure 7**). Although P-gp expression was decreased from 1.79% to 0.31% after treatment with 25 μM fludarabine, the effect was not significant, because the basal level of P-gp was low in EBV-negative NKL. In NK-92 cells, P-gp was downregulated by fludarabine in a dose-dependent manner. P-gp expression was 25% in the resting state and was decreased to 21.7%, 19.9% and 18.1% following treatment with 5, 12.5 and 25 μM fludarabine, respectively. However, the effect was not statistically significant. Additionally, in NK-YS cells, another EBV-positive cell line, inhibition of STAT1 signalling via fludarabine treatment decreased P-gp expression from 29.1% to 14.9% ($P < 0.05$). Altogether, we concluded that STAT1 phosphorylation has a close relationship with high P-gp expression and NecroX-5 downregulated P-gp expression through inhibition of the STAT1 signalling pathway more effective compared to fludarabine.

## Discussion

In this study, we first evaluated the direct relationships among EBV, ROS and P-gp. EBV infection caused hypoxic conditions, which in turn induced high levels of intracellular ROS. Increased intracellular ROS activated the STAT1 signalling pathway and phosphorylated STAT1 promoted P-gp expression resulting from *MDR1* gene translation (**Figure 8**). P-gp-induced drug efflux resulted in reduced chemosensitivity.

Interestingly, NecroX-5 regulated the expression and function of P-gp via intracellular ROS regulation and therefore increased chemosensitivity to the P-gp-dependent anti-cancer drugs doxorubicin and cisplatin.

Whether high levels of ROS aggravate tumor conditions is a subject of controversy [33-35]. It has been reported that EBV-induced ROS lead to a poor prognosis via signalling pathway modifications, gene instability and deregulation of enzymatic functions. Cerimele and colleagues first reported that high ROS levels aggravated EBV-positive Burkitt's lymphoma via VEGF production induced by MAPK phosphorylation [23]. EBNA1 promoted NF-κB activation by activating other viral genomes such as latent membrane protein 1 (LMP1), which is affected by highly expressed ROS levels [36] or ROS-induced EBV lytic gene expression via NF-κB and AP-1 signalling activation [22]. Additionally, there have been some reports that increased ROS levels after EBV infection promoted gene instability by DNA damage, inhibition of DNA repair [19] and telomere dysfunction [18]. Impairment of enzymes involved in intracellular ROS regulation, including malondialdehyde, catalase and superoxide dismutase, was reported in B cell lymphoma [15, 16] and in epithelial cells resulting in nasopharyngeal carcinomas [37-39]. In contrast, there are reports that upregulation of ROS induced tumor apoptosis and inhibited tumorigenesis in EBV-positive cancer. In EBV-infected B cells, high ROS expression induced apoptosis via centrocyte/centroblast marker 1 ligation [40] and Fas ligand upregulation by B7-H4 [41] and B7-H1 [42]. It has also been reported that intracellular ROS attenuated tumorigenesis via various signalling pathways, including the MAPK and JNK pathways [43-47], and activation of RhoA and Ras [48] and Tap73 and XAF1 [49]. Here, we demonstrated that high levels of intracellular ROS after EBV infection result in more aggressive tumor microenvironments.

In this study, we evaluated changes in various signalling pathway molecules including NF-κB, STAT and MAPK after NecroX-5 treatment to determine which signalling pathways are involved in the downregulation of P-gp by inhibiting intracellular ROS. As shown in **Figures 6** and **7**, we confirmed that inhibition of high phosphorylated STAT1 levels by NecroX-5 decreased P-gp expression, and STAT1 inhibition by the STAT1-specific inhibitor fludarabine downregulated P-gp *in vitro*. However, the mechanism about explaining why NecroX-5 is more effective than fludarabine remains to be studied. It has been reported that STAT1 phosphorylation is closely related to P-gp expression. Fryknas and colleagues first observed a higher level of phosphorylated STAT1 in doxorubicin-resistant myeloma cells [50]. In addition, in lung cancer, etoposide resistance was induced by P-gp expression regulated by histone deacetylase 4 at the transcriptional level and by STAT1 at the post-transcriptional level [51]. Therefore, NecroX-5 may also be effective against lung cancer, as ROS have been linked to oxidation and nuclear efflux of histone deacetylase 4. Although the role of STAT1 phosphorylation in cancer has recently proven controversial, as it can act as both a tumor suppressor and tumor promoter [52], our study is meaningful in confirming that STAT1 phosphorylation induced by ROS aggravated EBV-positive lymphoma via P-gp overexpression and NecroX-5 may serve as a new anti-cancer complement. However, in NK-YS cells, after treatment of NecroX-5, the phosphorylation of NF-κB was increased, we hypothesized that this seemed to be due to the changes of intracellular ROS environment, however, more research is needed to understand.

In conclusion, based on this study, EBV latent infection induced high levels of intracellular ROS and highly-induced ROS upregulated P-gp via the STAT1 signalling pathway. Interestingly, we confirmed that the ROS scavenger NecroX-5 regulated the expression and function of P-gp and pre-treatment of NecroX-5 to ENKTCL patients with hypoxic condition could increase therapeutic effects of existing P-gp-dependent anti-cancer drugs; therefore, NecroX-5 may be a novel anti-cancer drug complement to overcome resistance to anti-cancer drugs in EBV-positive NK cell lymphoma.

## Acknowledgements

This work was supported by a National Research Foundation of Korea (NRF) grant funded by the Korean government (MSIP) (No. NRF-2016R1A2B4007282).

## Disclosure of conflict of interest

None.

**Address correspondence to:** Dr. Seok-Goo Cho, Department of Hematology, Catholic Blood and Marrow Transplantation Center, Seoul St. Mary's Hospital, The Catholic University of Korea, College of Medicine, Seoul, Korea; Institute for Translational Research and Molecular Imaging, The Catholic University of Korea, College of Medicine, 222, Banpo-daero, Seocho-gu, Seoul 06591, Korea. Tel: 82-2-2258-6052; Fax: 82-2-599-3589; E-mail: chosg@catholic.ac.kr

## References

[1] Thorley-Lawson DA and Allday MJ. The curious case of the tumour virus: 50 years of Burkitt's lymphoma. Nat Rev Microbiol 2008; 6: 913-924.

[2] Cesarman E and Mesri EA. Kaposi sarcoma-associated herpesvirus and other viruses in human lymphomagenesis. Curr Top Microbiol Immunol 2007; 312: 263-287.

[3] Kutok JL and Wang F. Spectrum of Epstein-Barr virus-associated diseases. Annu Rev Pathol 2006; 1: 375-404.

[4] Tse E and Kwong YL. How I treat NK/T-cell lymphomas. Blood 2013; 121: 4997-5005.

[5] Metgud RS, Doshi JJ, Gaurkhede S, Dongre R and Karle R. Extranodal NK/T-cell lymphoma, nasal type (angiocentric T-cell lymphoma): a review about the terminology. J Oral Maxillofac Pathol 2011; 15: 96-100.

[6] Gill H, Liang RH and Tse E. Extranodal natural-killer/t-cell lymphoma, nasal type. Adv Hematol 2010; 2010: 627401.

[7] Karube K, Nakagawa M, Tsuzuki S, Takeuchi I, Honma K, Nakashima Y, Shimizu N, Ko YH, Morishima Y, Ohshima K, Nakamura S and Seto M. Identification of FOXO3 and PRDM1 as tumor-suppressor gene candidates in NK-cell neoplasms by genomic and functional analyses. Blood 2011; 118: 3195-3204.

[8] Iqbal J, Kucuk C, Deleeuw RJ, Srivastava G, Tam W, Geng H, Klinkebiel D, Christman JK, Patel K, Cao K, Shen L, Dybkaer K, Tsui IF, Ali H, Shimizu N, Au WY, Lam WL and Chan WC. Genomic analyses reveal global functional alterations that promote tumor growth and novel tumor suppressor genes in natural killer-cell malignancies. Leukemia 2009; 23: 1139-1151.

[9] Huang Y, de Leval L and Gaulard P. Molecular underpinning of extranodal NK/T-cell lymphoma. Best Pract Res Clin Haematol 2013; 26: 57-74.

[10] Yamaguchi M, Kita K, Miwa H, Nishii K, Oka K, Ohno T, Shirakawa S and Fukumoto M. Frequent expression of P-glycoprotein/MDR1 by nasal T-cell lymphoma cells. Cancer 1995; 76: 2351-2356.

[11] Lee J, Cho SG, Chung SM, Ryu MR, Kim SH, Jang HS and Choi BO. Retrospective analysis of treatment outcomes for extranodal NK/T-cell lymphoma (ENKL), nasal type, stage I-IIE: single institute experience of combined modality treatment for early localized nasal extranodal NK/T-cell lymphoma (ENKL). Ann Hematol 2013; 92: 333-343.

[12] Kim SY, Cho SG, Kim SW, Choi BO, Park KS, Lim J, Min CK, Kim YG, Lee JW and Min WS. Pilot study of pegylated interferon alpha-2a treatment during chemo- and radiotherapy and post-remission maintenance in patients with EBV-positive extranodal NK/T cell lymphoma. Ann Hematol 2011; 90: 693-699.

[13] Cho SG, Kim N, Sohn HJ, Lee SK, Oh ST, Lee HJ, Cho HI, Yim HW, Jung SE, Park G, Oh JH, Choi BO, Kim SW, Kim SW, Chung NG, Lee JW, Hong YS and Kim TG. Long-term outcome of extranodal NK/T cell lymphoma patients treated with postremission therapy using EBV LMP1 and LMP2a-specific CTLs. Mol Ther 2015; 23: 1401-1409.

[14] Sun J, Hu C, Zhu Y, Sun R, Fang Y, Fan Y and Xu F. LMP1 increases expression of NADPH Oxidase (NOX) and its regulatory subunit p22 in NP69 nasopharyngeal cells and makes them sensitive to a treatment by a NOX inhibitor. PLoS One 2015; 10: e0134896.

[15] Lassoued S, Ben Ameur R, Ayadi W, Gargouri B, Ben Mansour R and Attia H. Epstein-Barr virus induces an oxidative stress during the early stages of infection in B lymphocytes, epithelial, and lymphoblastoid cell lines. Mol Cell Biochem 2008; 313: 179-186.

[16] Gargouri B, Nasr R, ben Mansour R, Lassoued S, Mseddi M, Attia H, El Feki Ael F and Van Pelt J. Reactive oxygen species production and antioxidant enzyme expression after Epstein-Barr virus lytic cycle induction in Raji cell line. Biol Trace Elem Res 2011; 144: 1449-1457.

[17] Ohnishi S, Ma N, Thanan R, Pinlaor S, Hammam O, Murata M and Kawanishi S. DNA damage in inflammation-related carcinogenesis and cancer stem cells. Oxid Med Cell Longev 2013; 2013: 387014.

[18] Kamranvar SA and Masucci MG. The Epstein-Barr virus nuclear antigen-1 promotes telomere dysfunction via induction of oxidative stress. Leukemia 2011; 25: 1017-1025.

[19] Gruhne B, Sompallae R and Masucci MG. Three Epstein-Barr virus latency proteins independently promote genomic instability by inducing DNA damage, inhibiting DNA repair and inactivating cell cycle checkpoints. Oncogene 2009; 28: 3997-4008.

[20] Chen X, Kamranvar SA and Masucci MG. Oxidative stress enables Epstein-Barr virus-induced B-cell transformation by posttranscriptional regulation of viral and cellular grow-

th-promoting factors. Oncogene 2016; 35: 3807-3816.
[21] Ding Y, Zhu W, Sun R, Yuan G, Zhang D, Fan Y and Sun J. Diphenylene iodonium interferes with cell cycle progression and induces apoptosis by modulating NAD(P)H oxidase/ROS/cell cycle regulatory pathways in Burkitt's lymphoma cells. Oncol Rep 2015; 33: 1434-1442.
[22] De Leo A, Arena G, Lacanna E, Oliviero G, Colavita F and Mattia E. Resveratrol inhibits Epstein Barr Virus lytic cycle in Burkitt's lymphoma cells by affecting multiple molecular targets. Antiviral Res 2012; 96: 196-202.
[23] Cerimele F, Battle T, Lynch R, Frank DA, Murad E, Cohen C, Macaron N, Sixbey J, Smith K, Watnick RS, Eliopoulos A, Shehata B and Arbiser JL. Reactive oxygen signaling and MAPK activation distinguish Epstein-Barr Virus (EBV)-positive versus EBV-negative Burkitt's lymphoma. Proc Natl Acad Sci U S A 2005; 102: 175-179.
[24] Juliano RL and Ling V. A surface glycoprotein modulating drug permeability in Chinese hamster ovary cell mutants. Biochim Biophys Acta 1976; 455: 152-162.
[25] Ledoux S, Yang R, Friedlander G and Laouari D. Glucose depletion enhances P-glycoprotein expression in hepatoma cells: role of endoplasmic reticulum stress response. Cancer Res 2003; 63: 7284-7290.
[26] Ziemann C, Burkle A, Kahl GF and Hirsch-Ernst KI. Reactive oxygen species participate in mdr1b mRNA and P-glycoprotein overexpression in primary rat hepatocyte cultures. Carcinogenesis 1999; 20: 407-414.
[27] Seebacher NA, Richardson DR and Jansson PJ. Glucose modulation induces reactive oxygen species and increases P-glycoprotein-mediated multidrug resistance to chemotherapeutics. Br J Pharmacol 2015; 172: 2557-2572.
[28] Wartenberg M, Ling FC, Muschen M, Klein F, Acker H, Gassmann M, Petrat K, Putz V, Hescheler J and Sauer H. Regulation of the multidrug resistance transporter P-glycoprotein in multicellular tumor spheroids by hypoxia-inducible factor (HIF-1) and reactive oxygen species. FASEB J 2003; 17: 503-505.
[29] Yoshimori M, Takada H, Imadome K, Kurata M, Yamamoto K, Koyama T, Shimizu N, Fujiwara S, Miura O and Arai A. P-glycoprotein is expressed and causes resistance to chemotherapy in EBV-positive T-cell lymphoproliferative diseases. Cancer Med 2015; 4: 1494-1504.
[30] Kim HJ, Koo SY, Ahn BH, Park O, Park DH, Seo DO, Won JH, Yim HJ, Kwak HS, Park HS, Chung CW, Oh YL and Kim SH. NecroX as a novel class of mitochondrial reactive oxygen species and ONOO(-) scavenger. Arch Pharm Res 2010; 33: 1813-1823.
[31] Park J, Park E, Ahn BH, Kim HJ, Park JH, Koo SY, Kwak HS, Park HS, Kim DW, Song M, Yim HJ, Seo DO and Kim SH. NecroX-7 prevents oxidative stress-induced cardiomyopathy by inhibition of NADPH oxidase activity in rats. Toxicol Appl Pharmacol 2012; 263: 1-6.
[32] Im KI, Kim N, Lim JY, Nam YS, Lee ES, Kim EJ, Kim HJ, Kim SH and Cho SG. The free radical scavenger NecroX-7 attenuates acute graft-versus-host disease via reciprocal regulation of Th1/Regulatory T cells and inhibition of HMGB1 release. J Immunol 2015; 194: 5223-5232.
[33] Peiris-Pages M, Martinez-Outschoorn UE, Sotgia F and Lisanti MP. Metastasis and oxidative stress: are antioxidants a metabolic driver of progression? Cell Metab 2015; 22: 956-958.
[34] Sabharwal SS and Schumacker PT. Mitochondrial ROS in cancer: initiators, amplifiers or an Achilles' heel? Nat Rev Cancer 2014; 14: 709-721.
[35] Gupta SC, Hevia D, Patchva S, Park B, Koh W and Aggarwal BB. Upsides and downsides of reactive oxygen species for cancer: the roles of reactive oxygen species in tumorigenesis, prevention, and therapy. Antioxid Redox Signal 2012; 16: 1295-1322.
[36] Gruhne B, Sompallae R, Marescotti D, Kamranvar SA, Gastaldello S and Masucci MG. The Epstein-Barr virus nuclear antigen-1 promotes genomic instability via induction of reactive oxygen species. Proc Natl Acad Sci U S A 2009; 106: 2313-2318.
[37] Huang SY, Fang CY, Wu CC, Tsai CH, Lin SF and Chen JY. Reactive oxygen species mediate Epstein-Barr virus reactivation by N-methyl-N'-nitro-N-nitrosoguanidine. PLoS One 2013; 8: e84919.
[38] Cao JY, Mansouri S and Frappier L. Changes in the nasopharyngeal carcinoma nuclear proteome induced by the EBNA1 protein of Epstein-Barr virus reveal potential roles for EBNA1 in metastasis and oxidative stress responses. J Virol 2012; 86: 382-394.
[39] Huang SY, Fang CY, Tsai CH, Chang Y, Takada K, Hsu TY and Chen JY. N-methyl-N'-nitro-N-nitrosoguanidine induces and cooperates with 12-O-tetradecanoylphorbol-1,3-acetate/sodium butyrate to enhance Epstein-Barr virus reactivation and genome instability in nasopharyngeal carcinoma cells. Chem Biol Interact 2010; 188: 623-634.
[40] Kim YS, Park GB, Choi YM, Kwon OS, Song HK, Kang JS, Kim YI, Lee WJ and Hur DY. Ligation of centrocyte/centroblast marker 1 on Epstein-Barr virus--transformed B lymphocytes induces cell death in a reactive oxygen species--dependent manner. Hum Immunol 2006; 67: 795-807.

[41] Song H, Park G, Kim YS, Hur I, Kim H, Ryu JW, Lee HK, Cho DH, Choi IH, Lee WJ and Hur DY. B7-H4 reverse signaling induces the apoptosis of EBV-transformed B cells through Fas ligand up-regulation. Cancer Lett 2008; 266: 227-237.

[42] Kim YS, Park GB, Lee HK, Song H, Choi IH, Lee WJ and Hur DY. Cross-linking of B7-H1 on EBV-transformed B cells induces apoptosis through reactive oxygen species production, JNK signaling activation, and fasL expression. J Immunol 2008; 181: 6158-6169.

[43] Park GB, Bang SR, Lee HK, Kim D, Kim S, Kim JK, Kim YS and Hur DY. Ligation of CD47 induces G1 arrest in EBV-transformed B cells through ROS generation, p38 MAPK/JNK activation, and Tap73 upregulation. J Immunother 2014; 37: 309-320.

[44] Park GB, Choi Y, Kim YS, Lee HK, Kim D and Hur DY. ROS-mediated JNK/p38-MAPK activation regulates Bax translocation in Sorafenib-induced apoptosis of EBV-transformed B cells. Int J Oncol 2014; 44: 977-985.

[45] Park GB, Choi Y, Kim YS, Lee HK, Kim D and Hur DY. ROS and ERK1/2-mediated caspase-9 activation increases XAF1 expression in dexamethasone-induced apoptosis of EBV-transformed B cells. Int J Oncol 2013; 43: 29-38.

[46] Park GB, Kim YS, Lee HK, Song H, Kim S, Cho DH and Hur DY. Reactive oxygen species and p38 MAPK regulate Bax translocation and calcium redistribution in salubrinal-induced apoptosis of EBV-transformed B cells. Cancer Lett 2011; 313: 235-248.

[47] Park GB, Kim YS, Lee HK, Song H, Cho DH, Lee WJ and Hur DY. Endoplasmic reticulum stress-mediated apoptosis of EBV-transformed B cells by cross-linking of CD70 is dependent upon generation of reactive oxygen species and activation of p38 MAPK and JNK pathway. J Immunol 2010; 185: 7274-7284.

[48] Park GB, Kim YS, Song H, Kim S, Park DM, Lee WJ and Hur DY. Cross-linking of CD80 and CD86 diminishes expression of CD54 on EBV-transformed B cells through inactivation of RhoA and Ras. Immune Netw 2011; 11: 390-398.

[49] Park GB, Kim YS, Kim D, Kim S, Lee HK, Cho DH, Lee WJ and Hur DY. Melphalan-induced apoptosis of EBV-transformed B cells through upregulation of TAp73 and XAF1 and nuclear import of XPA. J Immunol 2013; 191: 6281-6291.

[50] Fryknas M, Dhar S, Oberg F, Rickardson L, Rydaker M, Goransson H, Gustafsson M, Pettersson U, Nygren P, Larsson R and Isaksson A. STAT1 signaling is associated with acquired crossresistance to doxorubicin and radiation in myeloma cell lines. Int J Cancer 2007; 120: 189-195.

[51] Kaewpiboon C, Srisuttee R, Malilas W, Moon J, Oh S, Jeong HG, Johnston RN, Assavalapsakul W and Chung YH. Upregulation of Stat1-HDAC4 confers resistance to etoposide through enhanced multidrug resistance 1 expression in human A549 lung cancer cells. Mol Med Rep 2015; 11: 2315-2321.

[52] Meissl K, Macho-Maschler S, Muller M and Strobl B. The good and the bad faces of STAT1 in solid tumours. Cytokine 2017; 89: 12-20.

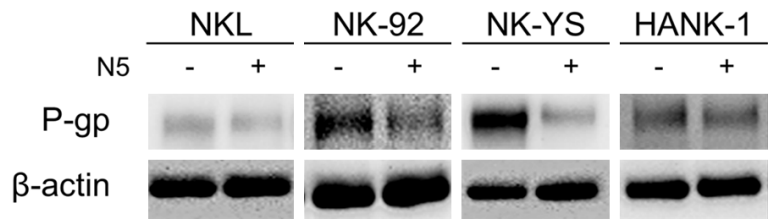


**Figure S1.** Reduction of P-gp expression after down-regulation of intracellular ROS using NecroX-5. Lymphoma cell lines were pre-treated with 20 μM NecroX-5 and cultured for protein expression. Total proteins were collected and western blot analyses for P-gp and β-actin were performed. In NK-92 and NK-YS cell lines, NecroX-5 was able to decrease P-gp expression significantly and in HANK-1 cell, P-gp expression was slightly reduced.